Chromophore twisting in the excited state of a photoswitchable fluorescent protein captured by time-resolved serial femtosecond crystallography

Nicolas Coquelle, Michel Sliwa, Joyce Woodhouse, Giorgio Schirò, Virgile Adam, Andrew Aquila, Thomas R. M. Barends, Sébastien Boutet, Martin Byrdin, Sergio Carbajo, et al.

Chromophore twisting in the excited state of a photoswitchable fluorescent protein captured by time-resolved serial femtosecond crystallography

Nicolas Coquelle[1†], Michel Sliwa[2†], Joyce Woodhouse[1†], Giorgio Schirò[1†], Virgile Adam[1†], Andrew Aquila[3], Thomas R. M. Barends[4], Sébastien Boutet[3], Martin Byrdin[1], Sergio Carbajo[3], Eugenio De la Mora[1], R. Bruce Doak[4], Mikolaj Feliks[1], Franck Fieschi[1], Lutz Foucar[4], Virginia Guillon[1], Mario Hilpert[4], Mark S. Hunter[3], Stefan Jakobs[5], Jason E. Koglin[3], Gabriela Kovacsova[4], Thomas J. Lane[3], Bernard Lévy[6], Mengning Liang[3], Karol Nass[4], Jacqueline Ridard[6], Joseph S. Robinson[3], Christopher M. Roome[4], Cyril Ruckebusch[2], Matthew Seaberg[3], Michel Thepaut[1], Marco Cammarata[7], Isabelle Demachy[6], Martin Field[1], Robert L. Shoeman[4], Dominique Bourgeois[1], Jacques-Philippe Colletier[1]*, Ilme Schlichting[4]* and Martin Weik[1]*

Chromophores absorb light in photosensitive proteins and thereby initiate fundamental biological processes such as photosynthesis, vision and biofluorescence. An important goal in their understanding is the provision of detailed structural descriptions of the ultrafast photochemical events that they undergo, in particular of the excited states that connect chemistry to biological function. Here we report on the structures of two excited states in the reversibly photoswitchable fluorescent protein rsEGFP2. We populated the states through femtosecond illumination of rsEGFP2 in its non-fluorescent off state and observed their build-up (within less than one picosecond) and decay (on the several picosecond timescale). Using an X-ray free-electron laser, we performed picosecond time-resolved crystallography and show that the hydroxybenzylidene imidazolinone chromophore in one of the excited states assumes a near-canonical twisted configuration halfway between the *trans* and *cis* isomers. This is in line with excited-state quantum mechanics/molecular mechanics and classical molecular dynamics simulations. Our new understanding of the structure around the twisted chromophore enabled the design of a mutant that displays a twofold increase in its off-to-on photoswitching quantum yield.

Fluorescent proteins (FPs) have revolutionized cellular imaging by serving as genetically encoded markers[1]. The propensity of FPs to fluoresce upon visible-light absorption or, alternatively, to relax via non-radiative pathways is largely dictated by the excited-state structural dynamics of the protein-embedded chromophore[2,3]. In solution, the isolated chromophore of the green fluorescent protein (GFP[4]) adopts a canonical 90° twisted geometry in the excited state[2] from which it reverts back to the planar ground state solely via radiationless decay[5]. The tight β-barrel scaffold of FPs restricts the conformational dynamics of the chromophore, which hinders radiationless decay and thus leads to an increase in the fluorescence quantum yield. Modulation of the chromophore twisting has been proposed to affect the photophysical properties of all FPs and has therefore been analysed by numerous theoretical and experimental studies[2,3,6–10].

A subgroup of FPs, the so-called reversibly photoswitchable fluorescent proteins (RSFPs)[11], can be toggled back and forth between a fluorescent (on) and a non-fluorescent (off) state. This property is of considerable interest for advanced fluorescence imaging and biotechnological developments[12]. Photoswitching in RSFPs is a two-step process that involves radiationless decay in the form of *cis*-to-*trans* or *trans*-to-*cis* isomerization and a change in the protonation state of the chromophore, as shown for asFP595[13], Dronpa[10,14,15], Padron[16] and IrisFP[17]. The structural basis of ultrafast events that lead to photoswitching and the order in which these proceed have so far remained elusive[18] as no crystallographic structure of an FP in an electronic excited state has been determined. Here we report the structural and spectroscopic characterization of excited states in rsEGFP2[19], an efficient tag in super-resolution microscopy, by the combined use of ultrafast transient absorption (TA) spectroscopy, time-resolved crystallography using an X-ray laser and excited-state quantum mechanics/molecular mechanics (QM/MM) and classical molecular dynamics (MD) simulations. Also, based on one of the excited-state structures, a mutant was designed that displays a twofold increase in off-to-on photoswitching quantum yield.

Results and discussion

Femtosecond TA spectroscopy of rsEGFP2 in solution. The chromophore of rsEGFP2 in its fluorescent on state (anionic *cis*

[1]Institut de Biologie Structurale, Univ. Grenoble Alpes, CEA, CNRS, F-38044 Grenoble, France. [2]Laboratoire de Spectrochimie Infrarouge et Raman, Université de Lille, CNRS, UMR 8516, LASIR, F59 000 Lille, France. [3]Linac Coherent Light Source (LCLS), SLAC National Accelerator Laboratory, 2575, Sand Hill Road, Menlo Park, California 94025, USA. [4]Max-Planck-Institut für medizinische Forschung, Jahnstrasse 29, 69120 Heidelberg, Germany. [5]Department of NanoBiophotonics, Max-Planck-Institut für biophysikalische Chemie, 37077 Göttingen, Germany. [6]Laboratoire de Chimie-Physique, CNRS/University Paris-Sud, University Paris-Saclay, UMR 8000, 91405 Orsay, France. [7]Department of Physics, University of Rennes 1, UMR UR1-CNRS 6251, Rennes, France. †These authors contributed equally to this work. *e-mail: martin.weik@ibs.fr; ilme.schlichting@mpimf-heidelberg.mpg.de; colletier@ibs.fr

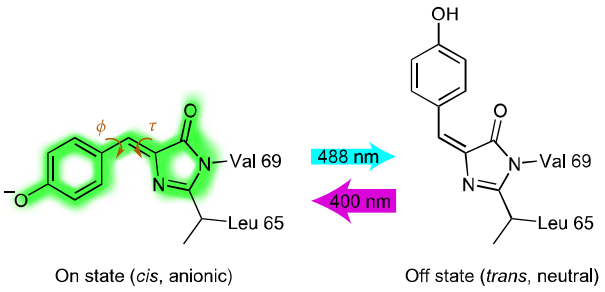

Figure 1 | Chromophore isomers and protonation states of rsEGFP2. The fluorescent on (*cis*/anionic) state is shown on the left and the non-fluorescent off (*trans*/neutral) state is shown on the right. The two dihedral angles τ and ϕ that bridge the phenol and imidazolinone rings are indicated by curved arrows (Supplementary Fig. 16c gives the atom numbering). On-to-off and off-to-on photoswitching is initiated by 488 and 400 nm light, respectively. The size of the coloured arrows visualizes the difference in switching quantum yields, which is an order of magnitude higher for the off-to-on photoswitching than for the reverse direction (Supplementary Table 7).

isomer) can be photoswitched to the non-fluorescent off state (protonated *trans* isomer) by irradiation at 488 nm (Fig. 1 and Supplementary Fig. 13). rsEGFP2 can then be toggled back to the on state by irradiation with 400 nm light. Here we focus on the off-to-on photoswitching, whose quantum yield is an order of magnitude higher than that of the on-to-off photoswitching (Supplementary Table 7). We used femtosecond TA spectroscopy to monitor spectral changes induced by excitation at 400 nm of the off-state rsEGFP2 in solution (Fig. 2 and Supplementary Fig. 1). Spectral changes appear within few hundreds of femtoseconds, reach a maximum close to 0.5 ps and decay on a timescale of several picoseconds (Fig. 2). At 0.5 ps two positive (maxima at 355 and 455 nm) and two negative bands (a narrow and a broad band with maxima at 405 and 530 nm, respectively) are observed. The former are characteristic of absorption by excited-state species, whereas the latter indicate depopulation of the off state (405 nm) and stimulated emission of excited-state species (530 nm). A global decay analysis was carried out, in which we focused on spectral changes observed at four wavelengths (385, 455, 530 and 650 nm). This analysis yielded three time constants, that is 90 fs, 0.9 ps and 3.7 ps (Fig. 2b). We attribute the first time constant to the build-up, from the Franck–Condon state, of two electronically excited intermediates, which respectively decay with 0.9 and 3.7 ps time constants to ground states—that is, either backward to the protonated *trans* isomer or forward to a still-protonated *cis* isomer. The decay of the stimulated emission band from 500 to 700 nm needed to be fitted with two exponentials, which implies necessarily that there are two excited-state species. That the *cis* isomer is still protonated is reflected by the appearance of a positive band at 380 nm (Supplementary Information gives the details). Similar transient spectra were obtained on similar timescales (Supplementary Fig. 1f–j) when measurements were performed in heavy (D_2O) instead of light (H_2O) water, which suggests that excited-state proton transfer (ESPT) is unlikely. Our transient spectroscopic data are thus consistent with *trans*-to-*cis* isomerization that occurs in the excited state within picoseconds, followed by ground-state proton transfer on a slower timescale (Fig. 3), in line with previous studies on Dronpa[10,20] and IrisFP[18].

Ground-state structures determined by static serial femtosecond crystallography. We investigated the geometry of the excited state experimentally by time-resolved serial femtosecond crystallography (TR-SFX) at an X-ray free-electron laser (XFEL), a method that can provide structural snapshots on the subpicosecond timescale[21,22]. First, to determine the on-state structure we collected static SFX data at room temperature on rsEGFP2 in the on state (reference dataset) from microcrystals (Supplementary Fig. 12) streamed across the X-ray beam using a liquid microjet. The room-temperature structure of rsEGFP2 in the off state was obtained from static SFX (laser-off data set) of microcrystals that were pre-illuminated prior to injection with 488 nm continuous-wave (CW) laser light in a custom-made inline device[23]. Careful analysis of electron-density maps calculated from the laser-off data set showed that it was necessary to include the on state at an occupancy of 10% in the model, and the remainder corresponded to the off state (Supplementary Information). As these occupancies are in line with the 90% pre-illumination efficiency orthogonally assessed by absorption spectroscopy (Supplementary Information), this serves as an internal control, and establishes that our data allow the identification of small subpopulations reliably. The rsEGFP2 off- and on-state structures, both refined against 1.7 Å resolution data (Supplementary Table 5), show the hydroxybenzylidene imidazolinone (HBI) chromophore in its *trans* and its *cis* isomer state, respectively, held by a central α-helix within a β-barrel typical of all FPs (Supplementary Figs 16–18). Conformational changes previously identified by synchrotron methods[24] that accompany HBI isomerization between the off and on states are clearly visible (Tyr146, Asn147, His149, Val151 and Tyr152).

Excited-state structures determined by TR-SFX. We then set out to visualize the ultrafast structural changes that occur after photoexcitation of the off state. We could not perform a pump-laser power titration because of the scarcity of the XFEL beam time. We decided to err on the high rather than on the low side and used a very high laser-power density of nominally 400 GW cm^{-2}. Our reasoning for this choice was that previous experiments[21,22] used a similar power density and that the spatial overlap of the pump-laser focus with the XFEL beam at the interaction region can decrease because of drifts. This was indeed observed during the experiment and caused a 2–5-fold reduction of the nominal value before manual realignment, which resulted in an actual power-density range between 80 and 400 GW cm^{-2}. rsEGFP2 microcrystals were pre-illuminated with 488 nm laser light to generate the off state and TR-SFX data were collected at pump–probe delays of 1 ps (laser-on-Δ1 ps data set) and 3 ps (laser-on-Δ3 ps data set) after pump-laser excitation at 400 nm to yield intermediate-state structures. These delays were chosen on the basis of the time course of the spectral changes observed in solution (Fig. 2b), which are close to their maximum at 1 ps, and have substantially decayed by 3 ps. A difference Fourier map was calculated at 1.9 Å resolution between the laser-on-Δ1 ps and laser-off data sets ($F_{obs}^{\text{laser-on-}\Delta 1\text{ps}} - F_{obs}^{\text{laser-off}}$), which revealed strong peaks on the chromophore and surrounding residues (Fig. 4b). The highest peaks are located on the imidazolinone ring of the chromophore, on the methylene bridge and, to a lesser extent, on the phenol ring (Fig. 4c,d and Supplementary Fig. 28). A strong negative peak is located on water molecule 17. The strongest positive peaks are compatible with the presence of two new chromophore conformers in the laser-on-Δ1 ps dataset (Fig. 4c,d and Supplementary Figs 23–25). The first conformer (model P (planar)) is very close to the off-state conformer, whereas the second (model T (twist)) is midway between the off- and on-state conformers (Fig. 4c,d, Supplementary Figs 23 and 25 and Supplementary Movie 1). Water molecule 17 is hydrogen bonded to the protonated phenol group of the chromophore both in the off state[19] and in model P, but not in model T, where instead the chromophore phenol oxygen forms a hydrogen bond with water

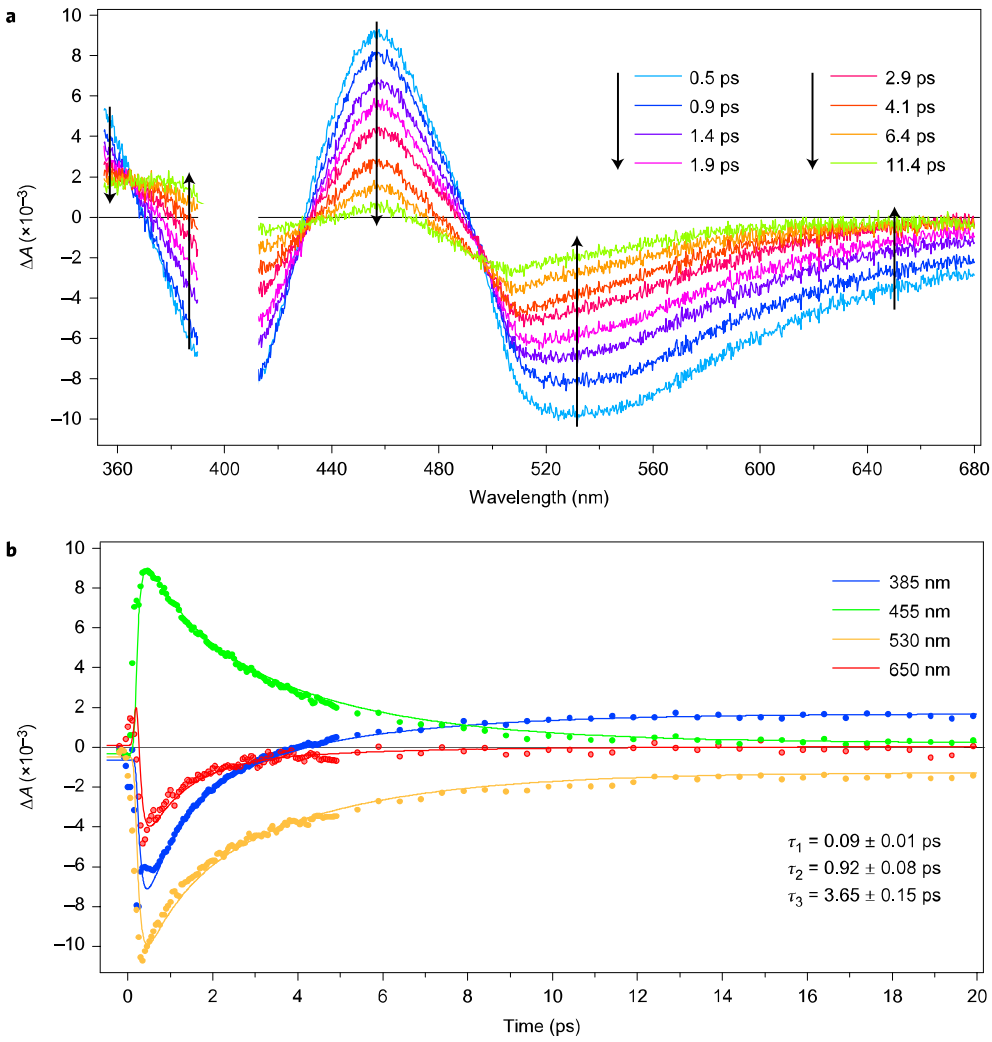

Figure 2 | Femtosecond TA spectroscopy of rsEGFP2 in solution. a, Femtosecond transient difference absorption spectra recorded at different time delays after a femtosecond laser excitation (400 nm) starting from the *trans* neutral off state. The spectrum without laser excitation was subtracted to calculate the difference spectrum. **b**, Kinetic traces at different wavelengths and the respective fit based on a global analysis with three exponential functions and a constant convoluted with a Gaussian-shaped pulse of 110 fs (full-width at half maximum). In these experiments, the pump-laser energy density was low enough (1.3 mJ cm^{-2}) to avoid multiphoton processes.

molecule 356. A total occupancy of 6–7% was estimated for these two conformers by two different approaches (Supplementary Information), which led us to perform difference refinement[25,26]. The laser-on-Δ1 ps data are best modelled by a combination of models P and T at relative occupancies of 0.6 and 0.4, respectively (Supplementary Information). A simulated difference Fourier map with the experimentally determined absolute occupancies of 4 and 3% for models P and T, respectively, reproduced the features in the $F_{obs}^{\text{laser-on-}\Delta 1\text{ps}} - F_{obs}^{\text{laser-off}}$ maps (Supplementary Information).

Structural changes that occur within 3 ps of photoexcitation were assessed by inspecting a $F_{obs}^{\text{laser-on-}\Delta 3\text{ps}} - F_{obs}^{\text{laser-off}}$ electron-density map (Fig. 4e,f) calculated at 1.9 Å resolution and comparing it with a $F_{obs}^{\text{laser-on-}\Delta 1\text{ps-random}} - F_{obs}^{\text{laser-off}}$ map calculated from data that consisted of the same number of randomly selected indexed images as used for the 1 ps data set (Supplementary Fig. 28b,c). Owing to the lower quality of the laser-on-Δ3 ps data set, we refrained from performing difference refinement and instead interpreted changes in the features of the difference Fourier map. At 3 ps, only model T is clearly consistent with the observed peaks (Fig. 4e,f and Supplementary Information). Integration of the peaks associated with model T in the $F_{obs}^{\text{laser-on-}\Delta 1\text{ps-random}} - F_{obs}^{\text{laser-off}}$ and $F_{obs}^{\text{laser-on-}\Delta 3\text{ps}} - F_{obs}^{\text{laser-off}}$ maps indicate a 44% decrease between 1 ps and 3 ps, which suggests that the intermediate state corresponding to model T has been partially depleted after 3 ps. There is no clear evidence for the presence of model P at 3 ps, either because the corresponding species has fully decayed or because the lower quality of the laser-on-Δ3 ps data set does not allow identification of an intermediate state so close to the off-state conformer. Positive peaks that overlap with the chromophore *cis* isomer are present in the $F_{obs}^{\text{laser-on-}\Delta 3\text{ps}} - F_{obs}^{\text{laser-off}}$ map (Fig. 4e,f and Supplementary Fig. 28b), but absent in the $F_{obs}^{\text{laser-on-}\Delta 1\text{ps}} - F_{obs}^{\text{laser-off}}$ map (Fig. 4c,d), which suggests that a fraction of the chromophores has isomerized at 3 ps, but not yet at 1 ps. In addition, the integration of negative peaks associated with the off-state *trans* chromophore maps reveal a 37% decrease between 1 ps and 3 ps. Thus, not only have intermediate states decayed after 3 ps, but ground states have also populated (*cis* isomer) and repopulated (off state).

Excited-state simulations. Photoinduced changes in chromophore conformation on the ultrafast timescale were also explored computationally by means of excited-state QM/MM and classical MD simulations. These were carried out starting from the static

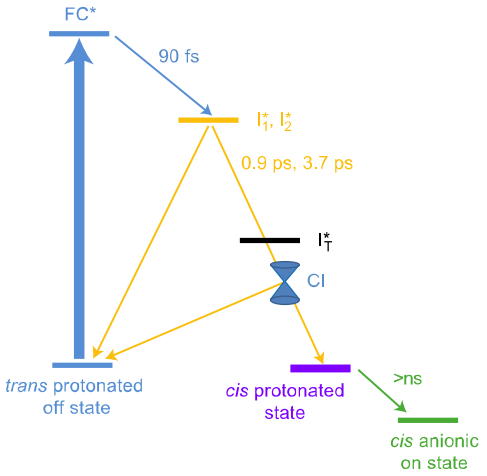

Figure 3 | Model for the off-to-on photoswitching of rsEGFP2. I_1^* and I_2^* are two excited-state species identified by TA spectroscopy. I_1^* corresponds to the twisted intermediate (model T) determined in the 1 ps time-delay SFX data and not detected by TA spectroscopy. Subpicosecond, picosecond and nano-to-millisecond processes are indicated by blue, yellow and green arrows, respectively. FC*, Franck–Condon state.

SFX structure of rsEGFP2 in its off state (laser-off data set). During a 100 ps simulation of the rsEGFP2 QM/MM system in its ground state (S_0), the ring-bridging dihedral angles of the chromophore, τ and ϕ (definitions in Fig. 1 and Supplementary Fig. 16c), remained close to those observed in the crystallographic off-state structure. Subsequently, trajectories of 2 ps duration in the S_1 excited state were spawned from the ground-state simulation at 1 ps intervals. Supplementary Fig. 8 (left panel) shows the values of the τ and ϕ angles as a function of time, averaged over 100 S_1 excited-state trajectories. On excitation, the τ and ϕ angles change rapidly from $4 \pm 8°$ and $-48 \pm 11°$ in the S_0 state to $-86 \pm 9°$ and $16 \pm 10°$ in the S_1 state (Fig. 4a). This leads to a twisted conformation of the chromophore with a perpendicular orientation of the phenol and imidazole groups (Supplementary Fig. 9a), in agreement with previous QM/MM studies on other RSFPs[27]. The change in chromophore conformation is essentially complete after 1 ps, a delay after which model T was observed in the TR-SFX experiments (Fig. 4a–d). Excited-state classical MD simulations were carried out as a complement to the QM/MM simulations (Supplementary Information). For the S_1 state they yielded a major chromophore conformation ($\tau = -73°$, $\phi = 11°$), similar to that found by excited-state QM/MM simulations, and an additional minor conformation ($\tau = -30°$, $\phi = -11°$) (Fig. 4a). The minor and major MD conformations are accessed, on average, in less than 30 fs and 1.9 ps, respectively. Both QM/MM and excited-state classical MD simulations thus yield for the electronically excited S_1 state a twisted chromophore conformation very similar to that of model T in the laser-on-Δ1 ps TR-SFX structure (Fig. 4a and Supplementary Fig. 9a).

Connection of species and conformations and off-to-on photoswitching model. The high pump-laser power density used in the TR-SFX experiments make the possibility that the crystallographically observed structural changes are caused or influenced by ionization, multiphoton and/or heating effects a legitimate concern, and at this time we cannot exclude this possibility. However, to address these concerns, we performed several additional calculations and experiments (Supplementary Information) that support our interpretation of the observed structural changes being representative of photoswitching intermediates: (1) the effect of multiphoton absorption on the structure was addressed by QM/MM calculations on the S_2 and S_3 excited states (Supplementary Information) that yielded a different conformation than the observed twisted conformation; (2) solution studies showed that off-to-on photoswitching is fully reversible after femtosecond laser excitation at the power density employed in the SFX experiments (Supplementary Fig. 7), making it unlikely that SFX model T corresponds to an irreversibly bleached species (however, it remains possible that multiphoton absorption results in a spectroscopically silent off-pathway intermediate); (3) importantly, time-resolved absorption spectroscopy of rsEGFP2 in solution provided circumstantial evidence that, indeed a cationic chromophore species forms at 68 GW cm^{-2} and 140 GW cm^{-2} (Supplementary Information and Supplementary Fig. 4). However, this species is stable on a timescale of nanoseconds, whereas the species that corresponds to SFX model T significantly decays between 1 and 3 ps in TR-SFX; (4) density functional theory (DFT) calculations of an ionized ground-state cation yielded a planar, not a twisted, chromophore. We cannot exclude that SFX model P could result from nonlinear excitation and corresponds to the cationic species. In conclusion, experimental and computational data altogether support the notion that the chromophore twisting observed by TR-SFX (model T) was not caused by ionization, irreversible photobleaching or multiphoton absorption.

The intermediate species and conformations detected by TA spectroscopy can be tentatively connected to those determined by TR-SFX and by simulations. In the refined SFX model T (Fig. 4c, d), the two ring-bridging dihedral angles τ and ϕ differ by ~90°, which results in a perpendicular positioning of the phenol and imidazolinone groups in a twisted chromophore (Supplementary Movie 1). This twisted conformation corresponds to that obtained by QM/MM and classical MD for the S_1 electronic excited state (Fig. 4a and Supplementary Fig. 9). Thus, SFX model T can be attributed to an S_1 intermediate species (denoted I_T^* in Fig. 3), but cannot correspond to either of the excited-state species identified by TA spectroscopy (I_1^* and I_2^* in Fig. 3), as the calculated transition dipole moment for model T is almost zero (not shown). A similar chromophore twisting in the excited state has been reported recently for PYP[22]. The chromophore conformation in the SFX model P (Fig. 4c,d) is similar to the minor conformation that is accessed in less than 30 fs in classical MD simulations of S_1 (Fig. 4a) and could correspond to one of the two TA spectroscopy species (I_1^* and I_2^*) characterized by a broad stimulated emission band at 530 nm (Fig. 2a). QM/MM calculations of the species with the highest transition dipole moment lead to a conformation (red star in Fig. 4a) close to SFX model P.

We present a tentative model for off-to-on photoswitching of rsEGFP2 (Fig. 3). Excitation of the *trans* protonated off state leads to a Franck–Condon state that relaxes in 90 fs to two excited-state species, I_1^* and I_2^*, as seen by TA spectroscopy, one of which corresponds to the nearly planar conformation of model P detected in TR-SFX at 1 ps. I_1^* and I_2^* decay in 0.9 and 3.7 ps, respectively, either backward to the *trans* protonated off state or forward to a *cis* protonated state, as evidenced by TR-SFX at 3 ps. We anticipate that the *cis* protonated state becomes deprotonated on a timescale beyond that of our TA spectroscopy experiments. The spectroscopically invisible twisted intermediate I_T^* observed in the TR-SFX, QM/MM and MD simulations is close to the conical intersection (CI) and is thus still electronically excited. The scheme illustrates the complementarity of TA spectroscopy and TR-SFX, which are sensitive to electronic and structural changes, respectively.

Chromophore twisting during the transition from the off-state to SFX model T involves changes in τ and ϕ of −84° and +43°, respectively. This supports that *trans*-to-*cis* isomerization during off-to-on photoswitching in rsEGFP2 proceeds via a hula-twist motion[28], in line with the mechanism proposed for asFP595[13]. Theoretical studies suggested that, on excitation, the protonated HBI chromophore preferentially rotates around τ, which would facilitate

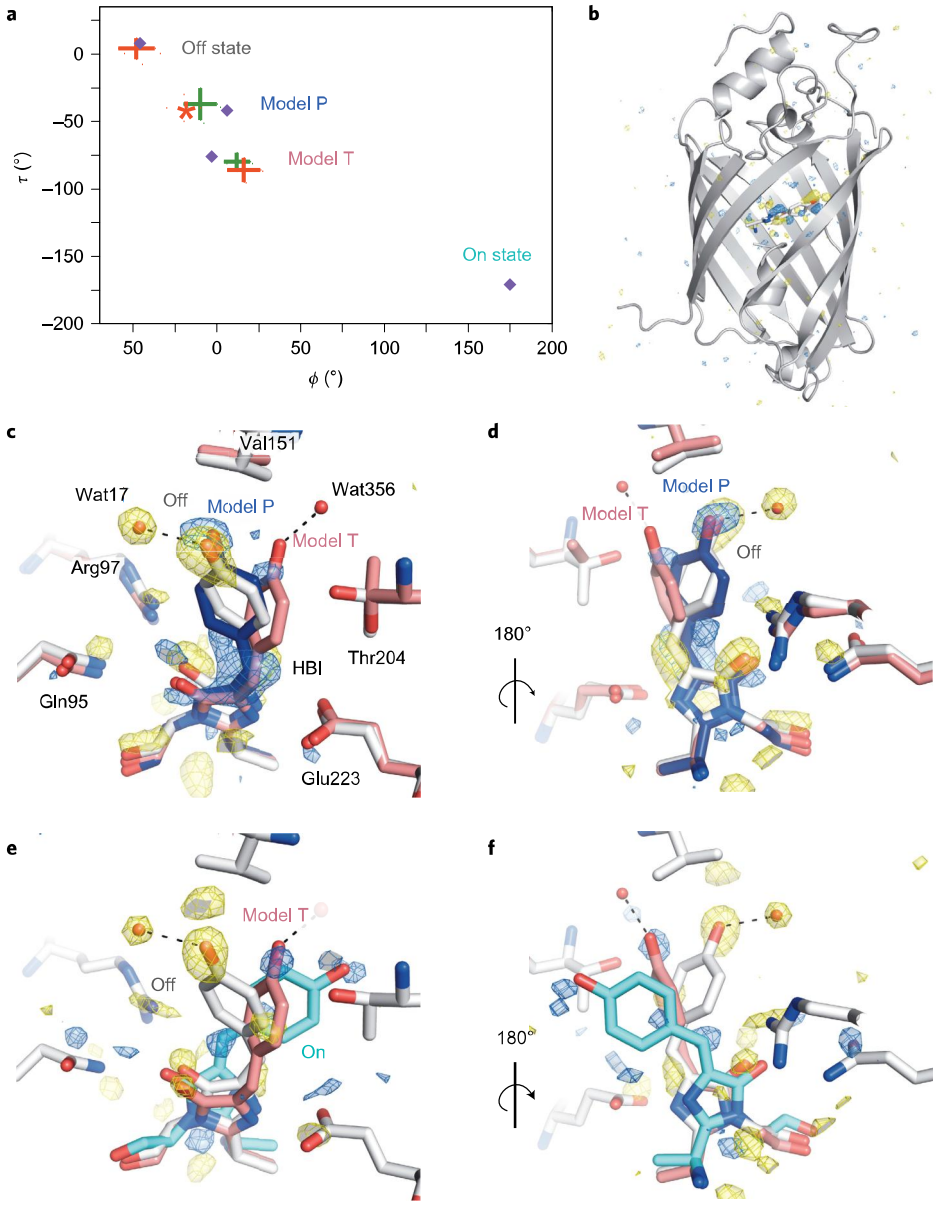

Figure 4 | rsEGFP2 in the electronically excited S_1 state. a, Ring-bridging τ and ϕ values for the crystallographically determined chromophore models (blue diamonds) and those determined by excited-state QM/MM simulations (red crosses) and excited-state MD simulations (green crosses). The size of the crosses corresponds to one standard deviation. The red star corresponds to the conformation with the largest transition dipole moment as calculated by QM/MM. **b–d**, Difference Fourier electron-density map $F_{obs}^{laser\text{-}on\text{-}\Delta 1ps} - F_{obs}^{laser\text{-}off}$, computed between the SFX data collected 1 ps after pump-laser excitation and without excitation, respectively, contoured at -3.5σ (yellow) and $+3.5\sigma$ (blue) shown for the entire protein (**b**) and zoomed into the chromophore region (**c** and **d**). In **b**, one strand of the β-barrel is omitted for clarity. In **c** and **d**, the chromophore models refined from the laser-off (grey) and laser-on-Δ1 ps (model T in pink, and model P in blue) datasets are shown, as well as residues that change conformation on the formation of model T. In the intermediate state, model T, the chromophore is twisted, with the phenol and the imidazolinone ring perpendicular to each other. **e**,**f**, Difference Fourier map $F_{obs}^{laser\text{-}on\text{-}\Delta 3ps} - F_{obs}^{laser\text{-}off}$, computed between SFX data collected 3 ps after pump-laser excitation and without excitation, respectively, contoured at -3.0σ (yellow) and $+3.0\sigma$ (blue). No model was produced from the laser-on-Δ3 ps data set. In **e** and **f**, models for the off (grey), the on (cyan) and the twisted (pink) chromophore (determined from the laser-on-Δ1 ps data set) are shown. All difference Fourier maps are Q-weighted[39]. Wat, water.

isomerization[8]. Although our data confirm that chromophore twisting involves a large change in τ, they also indicate that in rsEGFP2, the protein matrix tunes the relative amount of τ and ϕ rotations to minimize the energetic cost of *trans*-to-*cis* isomerizaton through the excited-state potential energy surface.

Protein structural changes accompanying chromophore twisting. The formation of the fully twisted intermediate state I_T^* involves substantial structural changes for residues of the chromophore-binding pocket (Supplementary Fig. 23). Three residues stand out, namely Arg97, which is hydrogen bonded to the chromophore imidazolinone ring in ground-state structures (off and on) but not in the twisted intermediate state, and Val151 and Thr204, which surround the phenol group (Fig. 4c,d). Most strikingly, Thr204 accompanies the isomerization of the chromophore to display different rotamers in the on state, the off state and the twisted intermediate state (Supplementary Fig. 23). In the twisted intermediate state, the chromophore phenol group and the Val151

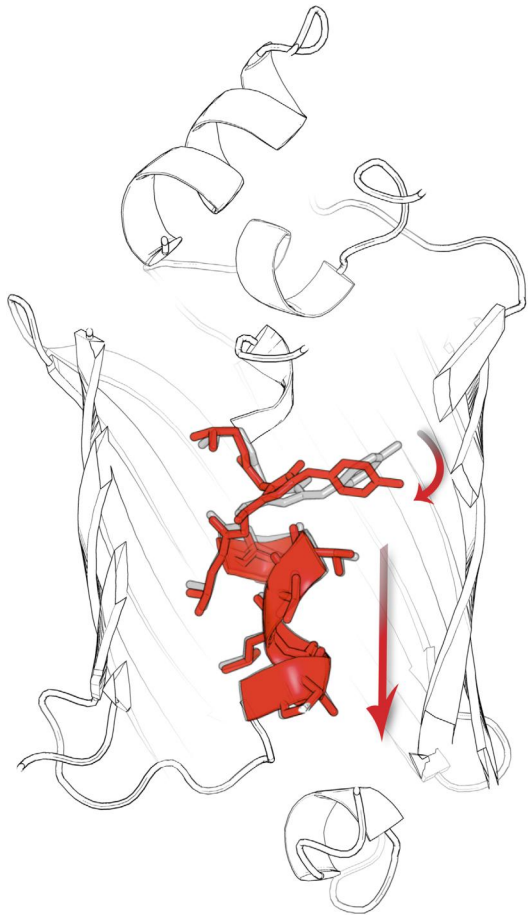

Figure 5 | Chromophore twisting is accompanied by a downward movement of the central α-helix along the barrel axis. The off state is shown in grey and the twisted intermediate in red. The corresponding difference electron density is shown in Supplementary Fig. 24.

side chain are in close proximity (3.1 Å between the phenol oxygen and CG1 atoms of the former and the latter, respectively). To avoid a steric clash of its phenol group with the side chain of Val151, the chromophore imidazolinone ring tilts by 18° in the opposite direction (positive and negative peaks on the chromophore O2 atom in Fig. 4d), which probably causes the observed motion of the α-helix N terminal to the chromophore downward along the barrel axis (Fig. 5), and away from β-strands 7 (residues 146–152) and 10 (residues 200–209) (Supplementary Fig. 27). Chromophore twisting thus seems to be constrained at the phenol, which leads to a downward movement of the α-helix that carries the chromophore base (Fig. 5).

Rational protein design based on excited-state structures. The ability of the protein scaffold to accommodate a fully twisted chromophore is probably a key determinant to enable photoswitching in RSFPs, compared to non-photoswitchable FPs in which full twisting of the confined chromophore is believed to be strongly restrained. The close proximity of Val151 to the twisted chromophore in the excited state (see above and Supplementary Movie 1) suggests that photoswitching of rsEGFP2 could be facilitated by reducing the side chain at position 151 by a mutation to alanine. Indeed, spectroscopic characterization revealed that the V151A variant has an off-to-on (on-to-off) photoswitching quantum yield of 0.77 (0.064) compared with 0.40 (0.043) for the wild-type (WT) protein (Supplementary Fig. 30 and Supplementary Table 7). Efforts to engineer FPs have been based, so far, on ground-state structures only[29,30]. The present work provides the first example of rationally improving a photoswitching property based on an excited-state structure. Subpicosecond time-resolved serial crystallography at XFEL sources is expected to provide novel and comprehensive insight into the excited-state intermediates in a variety of other FPs, with the hereby demonstrated potential for the rational design of enhanced variants.

Methods

Protein expression, purification and crystallization. The protein was expressed and purified essentially as described previously[24]. Microcrystals were obtained by seeding, starting from previously established conditions[24] (Supplementary Information gives the details).

Ultrafast TA spectroscopy. Ultrafast TA experiments were carried out on rsEGFP2 in 50 mM HEPES, 50 mM NaCl, pH 8, using a similar method as described elsewhere[18]. Briefly, a 1 kHz femtosecond TA set-up was used and the pump beam (400 nm, 100 fs pulse length) was obtained by doubling 800 nm fundamental pulses. rsEGFP2 in the off state, with an absorbance of about 0.1 at 400 nm (chamber thickness 0.25 mm), was irradiated continuously within a flow cell by 470 nm light to photoswitch the protein to the off state after excitation by the pump-laser beam. The instrument response function (110 fs full-width at half-maximum (FWHM)) was estimated from the stimulated Raman amplification signal (Supplementary Fig. 1a) and spectra were corrected from group-velocity dispersion. To avoid multiphoton processes, the data shown in Fig. 2 were collected at a low excitation-energy density (1.3 mJ cm^{-2}, which corresponded to a power density of 13 GW cm^{-2}). To address the question if the pump-laser energy density employed in the TR-SFX experiments (see below) leads to either the formation of ionized chromophore species or the irreversible formation of photobleached species[31], time-resolved and steady-state absorption spectra of rsEGFP2 in solution were recorded after femtosecond laser excitation at various pump-laser energy densities (Supplementary Information).

Pre-illumination of microcrystals, SFX data collection and processing and structure refinement. rsEGFP2 microcrystals (Supplementary Fig. 12) were photoswitched from the on to the off state within an inline pre-illumination device[23] (CW laser (488 nm) (Supplementary Fig. 14)) prior to injection with a liquid microjet into the microfocus chamber of the Coherent X-ray Imaging Instrument[32] at the Linac Coherent Light Source (LCLS). An optical pump X-ray probe scheme was used for data collection. The crystalline protein in its off state was photoexcited (400 nm, 230 fs pulse length, 940 μJ mm^{-2}, 400 GW cm^{-2}) 1 ps and 3 ps prior to interaction with the FEL beam (9.5 keV, 35 fs pulse length) to yield SFX data sets with 64,620 (laser-on-Δ1 ps) and 22,259 (laser-on-Δ3 ps) indexed diffraction patterns, respectively. A data set (laser-off, 65,097 indexed patterns) was collected by interleaving images without pump-laser excitation (but with pre-illumination) with the 1 ps time-delay light data. A reference data set was collected of rsEGFP2 in the on state (34,715 indexed patterns) from crystals that were neither pre-illuminated (488 nm) nor photoexcited with pump-laser illumination (400 nm). NanoPeakCell[33] and CASS[34,35] were used to identify crystal hits, find Bragg peaks and sort laser-on and laser-off images. Diffraction patterns were indexed and integrated with CrystFEL[36] (Supplementary Table 5). Room-temperature static structures of rsEGFP2 in the off state (worldwide PDB (wwPDB) accession code 5O8A) and the on state (wwPDB accession code 5O89) were determined by molecular replacement using phases from the respective cryostructures determined by synchrotron methods (PDB ID codes 5DTY and 5DTX, respectively[24]). Details on the partial *Q*-weighted difference-refinement procedure[25,26] used to determine models T and P from the laser-on-Δ1 ps data set are described in Supplementary Information. Extrapolated structure factors (defined by equation (1) in Supplementary Information) and the corresponding difference-refined excited-state structure of rsEGFP2 have been deposited in the wwPDB under accession code 5O8B. The experimental laser-on-Δ1 ps dataset and the corresponding composite structure of rsEGFP2 (83% off state, 10% on state, 4% model P, 3% model T) have been deposited in the wwPDB under accession code 5O8C.

Excited-state QM/MM simulations. Excited-state simulations were performed using fully solvated models of rsEGFP2 derived from the SFX structure of the off state determined in this work. Each model had approximately 34,000 atoms. Excitation was simulated by carrying out classical MD simulations with the neutral chromophore in its S_0 ground state, and then spawning trajectories with the chromophore switched to its S_1 excited state. A QM/MM method was used to describe the chromophore's potential energy surface, with the chromophore (45 atoms) in the QM region, and the remaining atoms of the protein and solvent in the MM region. Overall, 100 and 50 excited-state trajectories were generated and analysed in the QM/MM and MM simulations, respectively. These excited-state simulations were complemented by other techniques, including DFT and pK_a calculations. Full details are given in Supplementary Information.

Excited-state classical MD simulations. Classical molecular dynamics simulations were performed using specifically designed force fields that describe the potential energy surfaces of the ground state and of the first excited singlet state of the

chromophore, which accounts for the relation between the two torsion angles τ and ϕ (ref. 37) in the excited state (Supplementary Information). All the amino acids were taken in their standard protonation state at pH 7, except Glu223, which was protonated to allow hydrogen bonding with the N2 nitrogen atom of the chromophore. The protein was neutralized with Na^+ cations and solvated in a water box. Starting from the SFX structure of the off state, a simulation was run for the S_0 state at constant temperature (300 K) and pressure (1 atm). Simulations (50) of the S_1 state of 5 ps duration each were carried out starting from snapshots extracted from the S_0-state simulation and using a custom-made specific version[37] of the PMEMD module of AMBER[38].

Code availability. The custom-written CNS script used to calculate the Q-weighted structure factor amplitude difference Fourier maps is available from J.-P. Colletier on request.

References

1. Dean, K. M. & Palmer, A. E. Advances in fluorescence labeling strategies for dynamic cellular imaging. *Nat. Chem. Biol.* **10,** 512–523 (2014).
2. Weber, W., Helms, V., McCammon, J. A. & Langhoff, P. W. Shedding light on the dark and weakly fluorescent states of green fluorescent proteins. *Proc. Natl Acad. Sci. USA* **96,** 6177–6182 (1999).
3. Maddalo, S. L. & Zimmer, M. The role of the protein matrix in green fluorescent protein fluorescence. *Photochem. Photobiol.* **82,** 367–372 (2006).
4. Tsien, R. Y. The green fluorescent protein. *Ann. Rev. Biochem.* **67,** 509–544 (1998).
5. Voityuk, A. A., Michel-Beyerle, M. -E. & Rösch, N. Structure and rotation barriers for ground and excited states of the isolated chromophore of the green fluorescent protein. *Chem. Phys. Lett.* **296,** 269–276 (1998).
6. Fang, C., Frontiera, R. R., Tran, R. & Mathies, R. A. Mapping GFP structure evolution during proton transfer with femtosecond Raman spectroscopy. *Nature* **462,** 200–204 (2009).
7. Meech, S. R. Excited state reactions in fluorescent proteins. *Chem. Soc. Rev.* **38,** 2922–2934 (2009).
8. Olsen, S., Lamothe, K. & Martinez, T. J. Protonic gating of excited-state twisting and charge localization in GFP chromophores: a mechanistic hypothesis for reversible photoswitching. *J. Am. Chem. Soc.* **132,** 1192–1193 (2010).
9. Regis Faro, A. *et al.* Low-temperature chromophore isomerization reveals the photoswitching mechanism of the fluorescent protein Padron. *J. Am. Chem. Soc.* **133,** 16362–16365 (2011).
10. Warren, M. M. *et al.* Ground-state proton transfer in the photoswitching reactions of the fluorescent protein Dronpa. *Nat. Commun.* **4,** 1461 (2013).
11. Adam, V., Berardozzi, R., Byrdin, M. & Bourgeois, D. Phototransformable fluorescent proteins: future challenges. *Curr. Opin. Chem. Biol.* **20C,** 92–102 (2014).
12. Nienhaus, K. & Nienhaus, G. U. Fluorescent proteins for live-cell imaging with super-resolution. *Chem. Soc. Rev.* **43,** 1088–1106 (2014).
13. Andresen, M. *et al.* Structure and mechanism of the reversible photoswitch of a fluorescent protein. *Proc. Natl Acad. Sci. USA* **102,** 13070–13074 (2005).
14. Ando, R., Mizuno, H. & Miyawaki, A. Regulated fast nucleocytoplasmic shuttling observed by reversible protein highlighting. *Science* **306,** 1370–1373 (2004).
15. Andresen, M. *et al.* Structural basis for reversible photoswitching in Dronpa. *Proc. Natl Acad. Sci. USA* **104,** 13005–13009 (2007).
16. Andresen, M. *et al.* Photoswitchable fluorescent proteins enable monochromatic multilabel imaging and dual color fluorescence nanoscopy. *Nat. Biotechnol.* **26,** 1035–1040 (2008).
17. Adam, V. *et al.* Structural characterization of IrisFP, an optical highlighter undergoing multiple photo-induced transformations. *Proc. Natl Acad. Sci. USA* **105,** 18343–18348 (2008).
18. Colletier, J. P. *et al.* Serial femtosecond crystallography and ultrafast absorption spectroscopy of the photoswitchable fluorescent protein IrisFP. *J. Phys. Chem. Lett.* **7,** 882–887 (2016).
19. Grotjohann, T. *et al.* rsEGFP2 enables fast RESOLFT nanoscopy of living cells. *eLife* **1,** e00248 (2012).
20. Yadav, D. *et al.* Real-time monitoring of chromophore isomerization and deprotonation during the photoactivation of the fluorescent protein Dronpa. *J. Phys. Chem. B* **119,** 2404–2414 (2015).
21. Barends, T. R. *et al.* Direct observation of ultrafast collective motions in CO myoglobin upon ligand dissociation. *Science* **350,** 445–450 (2015).
22. Pande, K. *et al.* Femtosecond structural dynamics drives the *trans/cis* isomerization in photoactive yellow protein. *Science* **352,** 725–729 (2016).
23. Schiro, G., Woodhouse, J., Weik, M., Schlichting, I. & Shoeman, R. L. Simple and efficient system for photoconverting light-sensitive proteins in serial crystallography experiments. *J. Appl. Crystallogr.* **50,** 932–939 (2017).
24. El Khatib, M., Martins, A., Bourgeois, D., Colletier, J. P. & Adam, V. Rational design of ultrastable and reversibly photoswitchable fluorescent proteins for super-resolution imaging of the bacterial periplasm. *Sci. Rep.* **6,** 18459 (2016).
25. Terwilliger, T. C. & Berendzen, J. Difference refinement: obtaining differences between two related structures. *Acta Crystallogr. D* **51,** 609–618 (1995).
26. Colletier, J.-P. *et al.* Use of a 'caged' analogue to study the traffic of choline within acetylcholinesterase by kinetic crystallography. *Acta Crystallogr. D* **63,** 1115–1128 (2007).
27. Schafer, L. V., Groenhof, G., Boggio-Pasqua, M., Robb, M. A. & Grubmuller, H. Chromophore protonation state controls photoswitching of the fluoroprotein asFP595. *PLoS Comput. Biol.* **4,** e1000034 (2008).
28. Liu, R. S. Photoisomerization by hula-twist: a fundamental supramolecular photochemical reaction. *Acc. Chem. Res.* **34,** 555–562 (2001).
29. Goedhart, J. *et al.* Structure-guided evolution of cyan fluorescent proteins towards a quantum yield of 93%. *Nat. Commun.* **3,** 751 (2012).
30. Pandelieva, A. T. *et al.* Brighter red fluorescent proteins by rational design of triple-decker motif. *ACS Chem. Biol.* **11,** 508–517 (2016).
31. Hutchison, C. D. M. *et al.* Photocycle populations with femtosecond excitation of crystalline photoactive yellow protein. *Chem. Phys. Lett.* **654,** 63–71 (2016).
32. Liang, M. *et al.* The coherent X-ray imaging instrument at the Linac coherent light source. *J. Synchrotron Rad.* **22,** 514–519 (2015).
33. Coquelle, N. *et al.* Raster-scanning serial protein crystallography using micro- and nano-focused synchrotron beams. *Acta Crystallogr. D* **71,** 1184–1196 (2015).
34. Foucar, L. *et al.* CASS-CFEL-ASG software suite. *Comput. Phys. Commun.* **183,** 2207–2213 (2012).
35. Foucar, L. CFEL-ASG software suite (CASS): usage for free-electron laser experiments with biological focus. *J. Appl. Crystallogr.* **49,** 1336–1346 (2016).
36. White, T. A. *et al.* Crystallographic data processing for free-electron laser sources. *Acta Crystallogr. D* **69,** 1231–1240 (2013).
37. Jonasson, G. *et al.* Excited state dynamics of the green fluorescent protein on the nanosecond time scale. *J. Chem. Theory Comput.* **7,** 1990–1997 (2011).
38. Case, D. A. *et al. AMBER 10* (Univ. of California, 2008).
39. Ursby, T. & Bourgeois, D. Improved estimation of structure-factor difference amplitudes from poorly accurate data. *Acta Crystallogr. A* **53,** 564–575 (1997).

Acknowledgements

The study was supported by a grant from the CNRS (PEPS SASLELX) to M.W., and an ANR grant to M.W., M.C. and M.Sliwa (ANR-15-CE32-0004 BioXFEL). Use of LCLS, SLAC National Accelerator Laboratory, is supported by the US Department of Energy, Office of Science, Office of Basic Energy Sciences under Contract no. DE-AC02-76SF00515. We acknowledge support from the Max Planck Society. This work used the Multistep Protein Purification Platform (MP3) of the Grenoble Instruct Center (ISBG; UMS 3518 CNRS-CEA-UJF-EMBL) with support from FRISBI (ANR-10-INSB-05-02) and GRAL (ANR-10-LABX-49-01) within the Grenoble Partnership for Structural Biology (PSB). The Chevreul Institute (FR 2638), the Ministère de l'Enseignement Supérieur et de la Recherche, the Région Nord-Pas de Calais and FEDER are acknowledged for financial support. G.K. acknowledges support from the European Union under the program FP7-PEOPLE-2011-ITN NanoMem (project number 317079). J.W. acknowledges support from the CEA through the IRTELIS PhD program.

Author contributions

M.W., D.B., J.-P.C. and I.S. designed the research. S.J. provided the rsEGFP2 plasmid. J.W., V.A., V.G., M.T. and F.F. expressed and purified the WT protein. V.A. cloned, expressed and purified the protein variant and V.A. and D.B. analysed it. J.W., V.G. and I.S. carried out the microcrystallization. G.S. and M.B. spectroscopically characterized the microcrystals. R.L.S. and G.S. designed and optimized the pre-illumination device. M.Feliks and M.Field carried out the excited-state QM/MM simulations. J.R., M.L. and I.D. carried out the excited-state classical MD simulations. M.S. and C.R. carried out time-resolved absorption spectroscopy. M.C. and G.S. carried out the steady-state absorption spectroscopy with femtosecond excitation. N.C, M.Sliwa, J.W., V.A., A.A., T.R.M.B., S.B., S.C., E.D.I.M., R.B.D., L.F., M. Hilpert, M.S.Hunter, J.E.K., G.K., T.J.L., M.L., K.N., J.S.R., C.M.R., M.Seaberg, M.C., R.L.S., J.P.C., I.S. and M.W. carried out the SFX experiments. R.L.S, R.B.D. and G.K. performed sample injections. J.S.R. and M.C. aligned and controlled the pump laser. A.A., S.B., M.S. Hunter, J.E.K. and M.L. prepared and performed data collection. C.M.R., M.Hilpert, L.F., N.C., T.R.M.B. and J.-P.C. carried out the online SFX data processing. N.C. and J.-P.C. carried out the offline SFX data processing and structure refinement, with input from T.R.M.B., K.N., I.S., D.B. and M.W. J.-P.C., G.S., R.L.S., J.W., M.S., M.C., M.Field, J.R. and B.L. wrote the Supplementary Information with input from M.W., N.C., T.R.M.B., I.S. and D.B. M.W., D.B. and I.S. wrote the manuscript with input from T.R.M.B., M.Field, J.-P.C., M.S. and I.D.

Competing financial interests

The authors declare no competing financial interests.